

Convex recovery from interferometric measurements

Laurent Demanet and Vincent Jugnon*

July 2013

Abstract

This note formulates a deterministic recovery result for vectors x from quadratic measurements of the form $(Ax)_i \overline{(Ax)_j}$ for some left-invertible A . Recovery is exact, or stable in the noisy case, when the couples (i, j) are chosen as edges of a well-connected graph. One possible way of obtaining the solution is as a feasible point of a simple semidefinite program. Furthermore, we show how the proportionality constant in the error estimate depends on the spectral gap of a data-weighted graph Laplacian. Such quadratic measurements have found applications in phase retrieval, angular synchronization, and more recently interferometric waveform inversion.

Acknowledgments. The authors would like to thank Amit Singer for interesting discussions.

1 Introduction

The goal of this note is to formulate an analogue to certain quadratic systems of the well-known relative error bound

$$\frac{\|x - x_0\|}{\|x_0\|} \leq \kappa(A) \frac{\|e\|}{\|b\|} \quad (1)$$

for the least-squares solution of the overdetermined linear system $Ax = b$ with $b = Ax_0 + e$, and where $\kappa(A)$ is the condition number of A .

We consider complex quadratic measurements of $x \in \mathbb{C}^n$ of the form

$$B_{ij} = (Ax)_i \overline{(Ax)_j}, \quad (i, j) \in E, \quad (2)$$

for certain well-chosen couples of indices (i, j) , a scenario that we qualify as “interferometric”. This combination is special in that it is symmetric in x , and of rank 1 with respect to the indices i and j , hence the problem can be thought of as rank-1 symmetric matrix completion.

The regime that interests us is when the number m of measurements, i.e., of couples (i, j) in E , is comparable to the number n of unknowns. While phaseless measurements $b_i = |(Ax)_i|^2$ only admit recovery when A has very special structure – such as, being a tall random matrix with Gaussian i.i.d. entries [5, 9] – products $(Ax)_i \overline{(Ax)_j}$ for $i \neq j$ correspond to the idea of phase differences hence encode much more information. As a consequence, stable recovery occurs under very general conditions: left-invertibility of A and “connectedness” of set E of couples (i, j) . These conditions suffice to allow for m to be on the order of n . Various algorithms return x accurately up to a global phase; we mostly discuss variants of lifting with semidefinite relaxation in this paper. In contrast to other recovery results in matrix completion [18, 6], no randomness is needed in the

*Department of Mathematics, MIT. VJ is supported by the Earth Resources Laboratory at MIT. This work was also supported by AFOSR, ONR, NSF, Total SA, and the Alfred P. Sloan Foundation.

data model, and our proof technique involves elementary spectral graph theory rather than dual certification or uncertainty principles.

Our result is that an inequality of the form (1) still holds, but with the *square root of the spectral gap of a data-weighted graph Laplacian* in place of $\|b\|$ in the right-hand side. This spectral gap quantifies the connectedness of E , and has the proper homogeneity with respect to b .

1.1 Interferometry

In optical imaging, an interference fringe of two (possibly complex-valued) wavefields $f(t)$ and $g(t)$, where t is either a time or a space variable, is any combination of the form $|f(t) + g(t + t')|^2$. The sum is a result of the linearity of amplitudes in the fundamental equations of physics (such as Maxwell or Schrödinger), while the modulus squared is simply the result of a detector measuring intensities. The cross term $2\Re(f(t)\overline{g(t + t')})$ in the expansion of the square manifestly carries the information of destructive vs. constructive interference, hence is a continuous version of what we referred to earlier as an “interferometric measurement”.

In particular, when the two signals are sinusoidal at the same frequency, the interferometric combination highlights a phase difference. In astronomical interferometry, the delay t' is for instance chosen so that the two signals interfere constructively, yielding better resolution. Interferometric synthetic aperture radar (InSAR) is a remote sensing technique that uses the fringe from two datasets taken at different times to infer small displacements. In X-ray ptychography [19], imaging is done by undoing the interferometric combinations that the diffracted X-rays undergo from encoding masks. These are but three examples in a long list of applications.

Interferometry is also playing an increasingly important role in geophysical imaging, i.e., inversion of the elastic parameters of the portions of the Earth’s upper crust from scattered seismic waves. In this context however, the signals are often impulsive rather than monochromatic. As a result, it is more common to perform quadratic combinations of the Fourier transform of seismograms at different receivers, such as $|\hat{f}(\omega) + \hat{g}(\omega)|^2$. The cross-term involves $\hat{f}(\omega)\overline{\hat{g}(\omega)}$, the Fourier transform of the cross-correlation of f and g . It highlights a time lag in the case when f and g are impulses.

Cross-correlations have been shown to play an important role in imaging, mostly because of their stability to statistical fluctuations of a scattering medium [3] or an incoherent source [16, 11]. Though seismic interferometry is a vast research area [4, 22, 27, 21], explicit inversion of reflectivity parameters from interferometric data has to our knowledge only been considered in [10, 14]. Interferometric inversion offers great promise for model-robust imaging, i.e., recovery of reflectivity maps in a less-sensitive way on specific kinds of errors in the forward model.

Finally, interferometric measurements also play an important role in quantum optical imaging. See [20] for a nice solution to the inverse problem of recovering a scattering dielectric susceptibility from measurements of two-point correlation functions relative to two-photon entangled states.

1.2 Broader context and related work

The setting of this paper is discrete, hence we let i and j in place of either a time or frequency variable. We also specialize to $f = g$, and we let $f = Ax$ to possibly allow an explanation of the signal f by a linear forward model¹ A .

The link between products of the form $f\bar{g}$ and squared measurements $|f + g|^2$ goes both ways,

¹Such as scattering from a reflectivity profile x in the Born approximation, for which A is a wave equation Green’s function.

as shown by the polarization identity

$$f_i \overline{f_j} = \frac{1}{4} \sum_{k=1}^4 e^{-i\pi k/2} |f_i + e^{i\pi k/2} f_j|^2.$$

Hence any result of robust recovery of f , or x , from couples $f_i \overline{f_j}$, implies the same result for recovery from phaseless measurements of the form $|f_i + e^{i\pi k/2} f_j|^2$. This latter setting was precisely considered by Candès et al. in [5], where an application to X-ray diffraction imaging with a specific choice of masks is discussed. In [1], Alexeev et al. use the same polarization identity to design good measurements for phase retrieval, such that recovery is possible with $m = O(n)$.

Recovery of f_i from $f_i \overline{f_j}$ for some (i, j) when $|f_i| = 1$ (interferometric phase retrieval) can be seen as a special case of the problem of angular synchronization considered by Singer [23]. There, rotation matrices R_i are to be recovered (up to a global rotation) from measurements of relative rotations $R_i R_j^{-1}$ for some (i, j) . This problem has an important application to cryo-electron microscopy, where the measurements of relative rotations are further corrupted in an a priori unknown fashion (i.e., the set E is to be recovered as well). An impressive recovery result under a Bernoulli model of gross corruption, with a characterization of the critical probability, were recently obtained by Wang and Singer [25]. The spectrum of an adapted graph Laplacian plays an important role in their analysis [2], much as it does in this paper. Singer and Cucuringu also considered the angular synchronization problem from the viewpoint of rigidity theory [24]. For the similar problem of recovery of positions from relative distance, with applications to sensor network localization, see for instance [13].

The algorithmic approach considered in this paper for solving interferometric inversion problems is to formulate them via lifting and semidefinite relaxation. This idea was considered by many groups in recent years [7, 5, 13, 23, 26], and finds its origin in theoretical computer science [12].

1.3 Recovery of unknown phases

Let us start by describing the simpler problem of interferometric phase recovery, when $A = I$ and we furthermore assume $|x_i| = 1$. Given a vector $x_0 \in \mathbb{C}^n$ such that $|(x_0)_i| = 1$, a set E of pairs (i, j) , and noisy interferometric data $B_{ij} = (x_0)_i \overline{(x_0)_j} + \varepsilon_{ij}$, find a vector x such that

$$|x_i| = 1, \quad \sum_{(i,j) \in E} |x_i \overline{x_j} - B_{ij}| \leq \sigma, \quad (3)$$

for some $\sigma > 0$. Here and below, if no heuristic is provided for σ , we may cast the problem as a minimization problem for the misfit and obtain σ a posteriori.

The choice of the elementwise ℓ_1 norm over E is arbitrary, but convenient for the analysis in the sequel². We aim to find situations in which this problem has a solution x close to x_0 , up to a global phase. Notice that x_0 is feasible for (3), hence a solution exists, as soon as $\sigma \geq \sum_{(i,j) \in E} |\varepsilon_{ij}|$.

The relaxation by *lifting* of this problem is to find X (a proxy for xx^*) such that

$$X_{ii} = 1, \quad \sum_{(i,j) \in E} |X_{ij} - B_{ij}| \leq \sigma, \quad X \succeq 0, \quad (4)$$

then let x be the top eigenvector of X with $\|x\|^2 = n$.

²The choice of ℓ_1 norm as “least unsquared deviation” is central in [25] for the type of outlier-robust recovery behavior documented there.

The notation $X \succeq 0$ means that X is symmetric and positive semi-definite. Again, the feasibility problem (4) has at least one solution ($X_0 = x_0 x_0^*$) as soon as $\sigma \geq \sum_{i,j \in E} |\varepsilon_{ij}|$.

The set E generates edges of a graph $G = (V, E)$, where the nodes in V are indexed by i . Without loss of generality, we consider E to be symmetric. By convention, G does not contain loops, i.e., the diagonal $j = i$ is not part of E . (Measurements on the diagonal are not informative for the phase recovery problem, since $|(x_0)_i|^2 = 1$.)

The graph Laplacian on G is

$$L_{ij} = \begin{cases} d_i & \text{if } i = j; \\ -1 & \text{if } (i, j) \in E; \\ 0 & \text{otherwise,} \end{cases}$$

where d_i is the node degree $d_i = \sum_{j: (i,j) \in E} 1$. Observe that L is symmetric and $L \succeq 0$ by Gershgorin. Denote by $\lambda_1 \leq \lambda_2 \leq \dots \leq \lambda_n$ the eigenvalues of L sorted in increasing order. Then $\lambda_1 = 0$ with the constant eigenvector $v_1 = \frac{1}{\sqrt{n}}$. The second eigenvalue is zero if and only if G has two or more disconnected components. When $\lambda_2 > 0$, its value is a measure of connectedness of the graph. Note that $\lambda_n \leq 2d$ by Gershgorin again, where $d = \max_i d_i$ is the maximum degree.

Since $\lambda_1 = 0$, the second eigenvalue λ_2 is called the spectral gap. It is a central quantity in the study of expander graphs: it relates to

- the edge expansion (Cheeger constant, large if λ_2 is large);
- the degree of separation between any two nodes (small if λ_2 is large); and
- the speed of mixing of a random walk on the graph (fast if λ_2 is large).

More information about spectral graph theory can be found, e.g., in the lecture notes by Lovasz [17]. It is easy to show with interlacing theorems that adding an edge to E , or removing a node from V , both increase λ_2 . The spectral gap plays an important role in the following stability result.

In the sequel, we denote the componentwise ℓ_1 norm on the set E by $\|\cdot\|_1$.

Theorem 1. Assume $\|\varepsilon\|_1 + \sigma \leq n\lambda_2$, where λ_2 is the second eigenvalue of the graph Laplacian L on G . Any solution x of (3) or (4) obeys

$$\|x - e^{i\alpha} x_0\| \leq 4 \sqrt{\frac{\|\varepsilon\|_1 + \sigma}{\lambda_2}},$$

for some $\alpha \in [0, 2\pi)$.

Manifestly, recovery is exact (up to the global phase ambiguity) as soon as $\varepsilon = 0$ and $\sigma = 0$, provided $\lambda_2 \neq 0$, i.e., the graph G is connected. The easiest way to construct expander graphs (graphs with large λ_2) is to set up a probabilistic model with a Bernoulli distribution for each edge in an i.i.d. fashion, a model known as the Erdős-Rényi random graph. It can be shown that such graphs have a spectral gap bounded away from zero independently of n with $m = O(n \log n)$ edges.

A stronger result is available when the noise ε originates at the level of x_0 , i.e., $B = x_0 x_0^* + \varepsilon$ has the form $(x_0 + e)(x_0 + e)^*$.

Corollary 2. Assume $\varepsilon = (x_0 + e)(x_0 + e)^* - x_0 x_0^*$ and $\sigma \leq n\lambda_2$, where λ_2 is the second eigenvalue of the graph Laplacian L on G . Any solution x of (3) or (4) obeys

$$\|x - e^{i\alpha} x_0\| \leq 4 \sqrt{\frac{\sigma}{\lambda_2}} + \|e\|,$$

for some $\alpha \in [0, 2\pi)$.

Proof. Apply theorem 1 with $\varepsilon = 0$, $x_0 + e$ in place of x_0 , then use the triangle inequality. \square

In the setting of the corollary, problem (3) always has $x = x_0 + e$ as a solution, hence is feasible even when $\sigma = 0$.

Let us briefly review the eigenvector method for interferometric recovery. In [23], Singer proposed to use the eigenvector corresponding to the smallest eigenvalue of the (noisy) data-weighted graph Laplacian as an estimator of the vector of phases. A similar idea appears in the work of Montanari et al. as the first step of their OptSpace algorithm [15], and in the work of Chatterjee on universal thresholding [8]. In our setting, this means defining

$$(\tilde{\mathcal{L}})_{ij} = \begin{cases} d_i & \text{if } i = j; \\ -B_{ij} & \text{if } (i, j) \in E; \\ 0 & \text{otherwise,} \end{cases}$$

and letting $x = \tilde{v}_1 \sqrt{n}$ where v_1 is the unit-norm eigenvector of $\tilde{\mathcal{L}}$ with smallest eigenvalue. Denote by $\tilde{\lambda}_1 \leq \tilde{\lambda}_2 \leq \dots$ the eigenvalues of $\tilde{\mathcal{L}}$. The following result is known from [2], but we provide an elementary proof for completeness.

Theorem 3. *Assume $\|\varepsilon\| \leq \tilde{\lambda}_2/2$. Then the result x of the eigenvector method obeys*

$$\|x - e^{i\alpha} x_0\| \leq \sqrt{2n} \frac{\|\varepsilon\|}{\tilde{\lambda}_2},$$

for some $\alpha \in [0, 2\pi)$.

Alternatively, we may express the inequality in terms of λ_2 , the spectral gap of the noise-free Laplacian L defined earlier, by noticing³ that $\tilde{\lambda}_2 \geq \lambda_2 - \|\varepsilon\|$. Both λ_2 and $\tilde{\lambda}_2$ are computationally accessible. In the case when $|B_{ij}| = 1$, we have $\tilde{\lambda}_1 \geq 0$, hence $\tilde{\lambda}_2$ is (slightly) greater than the spectral gap $\lambda_2 - \tilde{\lambda}_1$ of $\tilde{\mathcal{L}}$. Note that the $1/\tilde{\lambda}_2$ scaling appears to be sharp in view of the numerical experiments reported in section 3. The inverse square root scaling of theorem 1 is stronger in the presence of small spectral gaps, but the noise scaling is weaker in theorem 1 than in theorem 3.

1.4 Interferometric recovery

The more general version of the interferometric recovery problem is to consider a left-invertible tall matrix A , linear measurements $b = Ax_0$ for some vector x_0 (without condition on the modulus of either b_i or $(x_0)_i$), noisy interferometric measurements $B_{ij} = b_i \bar{b}_j + \varepsilon_{ij}$ for (i, j) in some set E , and find x subject to

$$\sum_{(i,j) \in E \cup D} |(Ax)_i \overline{(Ax)_j} - B_{ij}| \leq \sigma. \quad (5)$$

Notice that we now take the union of the diagonal $D = \{(i, i)\}$ with E . Without loss of generality we assume that $\varepsilon_{ij} = \overline{\varepsilon_{ji}}$, which can be achieved by symmetrizing the measurements.

Since we no longer have a unit-modulus condition, the relevant notion of graph Laplacian is now data-dependent. It reads

$$(L_{|b|})_{ij} = \begin{cases} \sum_{k: (i,k) \in E} |b_k|^2 & \text{if } i = j; \\ -|b_i| |b_j| & \text{if } (i, j) \in E; \\ 0 & \text{otherwise.} \end{cases}$$

³This owes to $\|\mathcal{L} - \tilde{\mathcal{L}}\| \leq \|\varepsilon\|$, with $\mathcal{L} = \Lambda L \Lambda^*$ the noise-free Laplacian with phases introduced at the beginning of section 2.1.

The connectedness properties of the underlying graph now depend on the size of $|b_i|$: the edge (i, j) carries valuable information if and only if both $|b_i|$ and $|b_j|$ are large.

A few different recovery formulations arise naturally in the context of lifting and semidefinite relaxation.

- The basic lifted formulation is to find some X such that

$$\sum_{(i,j) \in E \cup D} |(AXA^*)_{ij} - B_{ij}| \leq \sigma, \quad X \succeq 0,$$

then let $x = x_1 \sqrt{\eta_1}$, where (η_1, x_1) is the top eigen-pair of X . (6)

Our main result is as follows.

Theorem 4. Assume $\|\varepsilon\|_1 + \sigma \leq \lambda_2/2$, where λ_2 is the second eigenvalue of the data-weighted graph Laplacian $L_{|b|}$. Any solution x of (6) obeys

$$\frac{\|x - e^{i\alpha} x_0\|}{\|x_0\|} \leq 15 \kappa(A)^2 \sqrt{\frac{\|\varepsilon\|_1 + \sigma}{\lambda_2}},$$

for some $\alpha \in [0, 2\pi)$, and where $\kappa(A)$ is the condition number of A .

The quadratic dependence on $\kappa(A)$ is necessary⁴. In section 3, we numerically verify the inverse square root scaling in terms of λ_2 . The numerical experiments also indicate that the noise scaling is not in general tight – we do not know whether this is a consequence of the choice of regularization to pick a solution in the feasibility set or not.

If the noise originates from $b + e$ rather than $bb^* + \varepsilon$, the error bound is again improved to

$$\frac{\|x - e^{i\alpha} x_0\|}{\|x_0\|} \leq 15 \kappa(A)^2 \sqrt{\frac{\sigma}{\lambda_2}} + \kappa(A) \frac{\|e\|}{\|b\|},$$

for the same reason as earlier.

- An alternative, two-step lifting formulation is to find x through Y such that

$$\sum_{(i,j) \in E \cup D} |Y_{ij} - B_{ij}| \leq \sigma, \quad Y \succeq 0,$$

then let $x = A^+ y_1 \sqrt{\eta_1}$, where (η_1, y_1) is the top eigen-pair of Y . (7)

The dependence on the condition number of A is more favorable than for the basic lifting formulation.

Theorem 5. Assume $\|\varepsilon\|_1 + \sigma \leq \lambda_2/2$, where λ_2 is the second eigenvalue of the data-weighted graph Laplacian $L_{|b|}$. Any solution x of (5) or (7) obeys

$$\frac{\|x - e^{i\alpha} x_0\|}{\|x_0\|} \leq 15 \kappa(A) \sqrt{\frac{\|\varepsilon\|_1 + \sigma}{\lambda_2}},$$

for some $\alpha \in [0, 2\pi)$.

⁴ The following example shows why that is the case. For any X_0 and invertible A , the solution to $AXA^* = AX_0A^* + \varepsilon$ is $X = X_0 + A^+ \varepsilon (A^+)^+$. Let $X_0 = e_1 e_1^T$, $\varepsilon = \delta e_1 e_1^*$ for some small δ , and $A^+ = I + N e_1 e_1^T$. Then $X = (1 + \delta N^2) e_1 e_1^T$, and the square root of its leading eigenvalue is $\sqrt{\eta_1} \simeq 1 + \frac{1}{2} \delta N^2$. As a result, x is a perturbation of x_0 by a quantity of magnitude $O(\delta \|A^+\|^2)$.

The quantity λ_2 is not computationally accessible in general, but it can be related to the second eigenvalue $\tilde{\lambda}_2$ of the noisy data-weighted Laplacian,

$$\left(\tilde{\mathcal{L}}_B\right)_{ij} = \begin{cases} \sum_{k:(i,k) \in E} B_{kk} & \text{if } i = j; \\ -B_{ij} & \text{if } (i, j) \in E; \\ 0 & \text{otherwise.} \end{cases}$$

It is straightforward to show that $\lambda_2 \geq \tilde{\lambda}_2 - [(d+1)\|\varepsilon\|_\infty + \|\varepsilon\|]$, where $\|\cdot\|_\infty$ is the elementwise maximum on $E \cup D$, $\|\cdot\|$ is the spectral norm, and d is the maximum node degree.

2 Proofs

2.1 Proof of theorem 1.

Observe that if x is feasible for (3), then xx^* is feasible for (4), and has $e^{i\alpha}x$ as leading eigenvector. Hence we focus without loss of generality on (4).

As in [23], consider the Laplacian matrix weighted with the unknown phases,

$$\mathcal{L} = \Lambda \Lambda^*,$$

with $\Lambda = \text{diag}(x_0)$. In other words $\mathcal{L}_{ij} = (X_0)_{ij} L_{ij}$ with $X_0 = x_0 x_0^*$. We still have $\mathcal{L} \succeq 0$ and $\lambda_1 = 0$, but now $v_1 = \frac{1}{\sqrt{n}} x_0$. Here and below, λ and v refer to \mathcal{L} , and v has unit ℓ_2 norm.

The idea of the proof is to compare X with the rank-1 spectral projectors $v_j v_j^*$ of \mathcal{L} . Let $\langle A, B \rangle = \text{tr}(AB^*)$ be the Frobenius inner product. Any X obeying (3) can be written as $X = X_0 + \tilde{\varepsilon}$ with $\|\tilde{\varepsilon}\|_1 \leq \|\varepsilon\|_1 + \sigma$. We have

$$\langle X, \mathcal{L} \rangle = \langle X_0, \mathcal{L} \rangle + \langle \tilde{\varepsilon}, \mathcal{L} \rangle$$

A short computation shows that

$$\begin{aligned} \langle X_0, \mathcal{L} \rangle &= \sum_i (X_0)_{ii} \overline{\mathcal{L}_{ii}} + \sum_{(i,j) \in E} (X_0)_{ij} \overline{\mathcal{L}_{ij}} \\ &= -\sum_i d_i + \sum_{(i,j) \in E} (x_0)_i \overline{(x_0)_j} \overline{(x_0)_i} (x_0)_j \\ &= \sum_i \left[-d_i + \sum_{j:(i,j) \in E} 1 \right] \\ &= 0. \end{aligned}$$

Since $|L_{ij}| = 1$ on E , the error term is simply bounded as

$$|\langle \tilde{\varepsilon}, \mathcal{L} \rangle| \leq \|\tilde{\varepsilon}\|_1$$

On the other hand the Laplacian expands as

$$\mathcal{L} = \sum_j v_j \lambda_j v_j^*,$$

so we can introduce a convenient normalization factor $1/n$ and write

$$\left\langle \frac{X}{n}, \mathcal{L} \right\rangle = \sum_j c_j \lambda_j, \tag{8}$$

with

$$c_j = \left\langle \frac{X}{n}, v_j v_j^* \right\rangle = \frac{v_j^* X v_j}{n}.$$

Notice that $c_j \geq 0$ since we require $X \succeq 0$. Their sum is

$$\sum_j c_j = \left\langle \frac{X}{n}, \sum_j v_j v_j^* \right\rangle = \left\langle \frac{X}{n}, I \right\rangle = \frac{\text{tr}(X)}{n} = 1.$$

Hence (8) is a convex combination of the eigenvalues of \mathcal{L} , bounded by $\|\tilde{\varepsilon}\|_1/n$. The smaller this bound, the more lopsided the convex combination toward λ_1 , i.e., the larger c_1 . The following lemma makes this observation precise.

Lemma 1. *Let $\mu = \sum_j c_j \lambda_j$ with $c_j \geq 0$, $\sum_j c_j = 1$, and $\lambda_1 = 0$. If $\mu \leq \lambda_2$, then*

$$c_1 \geq 1 - \frac{\mu}{\lambda_2}.$$

Proof of lemma 1.

$$\mu = \sum_{j \geq 2} c_j \lambda_j \geq \lambda_2 \sum_{j \geq 2} c_j = \lambda_2(1 - c_1),$$

then isolate c_1 . □

Assuming $\|\tilde{\varepsilon}\|_1 \leq n\lambda_2$, we now have

$$\left\langle \frac{X}{n}, v_1 v_1^* \right\rangle \geq 1 - \frac{\|\tilde{\varepsilon}\|_1}{n\lambda_2}.$$

We can further bound

$$\begin{aligned} \left\| \frac{X}{n} - v_1 v_1^* \right\|_F^2 &= \text{tr} \left[\left(\frac{X}{n} - v_1 v_1^* \right)^2 \right] \\ &= \text{tr}((v_1 v_1^*)^2) + \frac{\text{tr}(X^2)}{n^2} - 2 \text{tr} \left(\frac{X}{n} v_1 v_1^* \right). \end{aligned}$$

The first term is 1. The second term is less than 1, since $\text{tr}(X^2) \leq \text{tr}(X)^2$ for positive semidefinite matrices. Therefore,

$$\left\| \frac{X}{n} - v_1 v_1^* \right\|_F^2 \leq 2 - 2 \text{tr} \left(\frac{X}{n} v_1 v_1^* \right) \leq \frac{2\|\tilde{\varepsilon}\|_1}{n\lambda_2}.$$

We can now control the departure of the top eigenvector of X/n from v_1 by the following lemma. It is analogous to the sin theta theorem of Davis-Kahan, except for the choice of normalization of the vectors. (It is also a generalization of a lemma used by one of us in [9] (section 4.2).) The proof is only given for completeness.

Lemma 2. *Consider any Hermitian $X \in \mathbb{C}^{n \times n}$, and any $v \in \mathbb{C}^n$, such that $\|X - vv^*\| < \frac{\|v\|^2}{2}$. Let η_1 be the leading eigenvalue of X , and x_1 the corresponding unit-norm eigenvector. Let x be defined either as (a) $x_1 \|v\|$, or as (b) $x_1 \sqrt{\eta_1}$. Then*

$$\|x\|x\| - e^{i\alpha} v \|v\| \| \leq 2\sqrt{2} \|X - vv^*\|,$$

for some $\alpha \in [0, 2\pi)$.

Proof of Lemma 2. Let $\delta = \|X - vv^*\|$. Notice that $\|vv^*\| = \|v\|^2$. Decompose $X = \sum_{j=1}^n x_j \eta_j x_j^*$ with eigenvalues η_j sorted in decreasing order. By perturbation theory for symmetric matrices (Weyl's inequalities),

$$\max\{|\|v\|^2 - \eta_1|, |\eta_2|, \dots, |\eta_n|\} \leq \delta, \quad (9)$$

so it is clear that $\eta_1 > 0$, and that the eigenspace of η_1 is one-dimensional, as soon as $\delta < \frac{\|v\|^2}{2}$.

Let us deal first with the case (a) when $x = x_1 \|v\|$. Consider

$$vv^* - xx^* = vv^* - X + Y,$$

where

$$Y = x_1(\|v\|^2 - \eta_1)x_1^* + \sum_{j=2}^n x_j \eta_j x_j^*.$$

From (9), it is clear that $\|Y\| \leq \delta$. Let $v_1 = v/\|v\|$. We get

$$\|vv^* - xx^*\| \leq \|vv^* - X\| + \|Y\| \leq 2\delta.$$

Pick α so that $|v^*x| = e^{-i\alpha}v^*x$. Then

$$\begin{aligned} \|v\|v - e^{-i\alpha}x\|x\| \|^2 &= \|v\|^4 + \|x\|^4 - 2\|v\|\|x\|\Re e^{-i\alpha}v^*x \\ &= \|v\|^4 + \|x\|^4 - 2\|v\|\|x\||v^*x| \quad \text{by definition of } \alpha \\ &\leq \|v\|^4 + \|x\|^4 - 2|v^*x|^2 \quad \text{by Cauchy-Schwarz} \\ &= \|vv^* - xx^*\|_F^2 \\ &\leq 2\|vv^* - xx^*\|^2 \quad \text{because } vv^* - xx^* \text{ has rank 2} \\ &\leq 8\delta^2. \end{aligned}$$

The case (b) when $x = x_1\sqrt{\eta_1}$ is treated analogously. The only difference is now that

$$Y = \sum_{j=2}^n x_j \eta_j x_j^*.$$

A fortiori, $\|Y\| \leq \delta$ as well. □

Part (a) of lemma 2 is applied with X/n in place of X , and v_1 in place of v . In that case, $\|v_1\| = 1$. We conclude the proof by noticing that $v_1 = \frac{x_0}{\sqrt{n}}$, and that the output x of the lifting method is normalized so that $x_1 = \frac{x}{\sqrt{n}}$.

2.2 Proof of theorem 3

The proof is a simple argument of perturbation of eigenvectors. We either assume $\varepsilon_{ij} = \overline{\varepsilon_{ji}}$ or enforce it by symmetrizing the measurements. Define \mathcal{L} as previously, and notice that $\|\mathcal{L} - \tilde{\mathcal{L}}\| \leq \|\varepsilon\|$. Consider the eigen-decompositions

$$\mathcal{L}v_j = \lambda_j v_j, \quad \tilde{\mathcal{L}}\tilde{v}_j = \tilde{\lambda}_j \tilde{v}_j,$$

with $\lambda_1 = 0$. Form

$$\tilde{\mathcal{L}}v_j = \lambda_j v_j + r_j,$$

with $\|r_j\| \leq \|\varepsilon\|$. Take the dot product of the equation above with \tilde{v}_k to obtain

$$\langle \tilde{v}_k, r_j \rangle = (\tilde{\lambda}_k - \lambda_j) \langle \tilde{v}_k, v_j \rangle.$$

Let $j = 1$, and use $\lambda_1 = 0$. We get

$$\sum_{k \geq 2} |\langle \tilde{v}_k, v_1 \rangle|^2 \leq \frac{\sum_{k \geq 2} |\langle \tilde{v}_k, r_1 \rangle|^2}{\min_{k \geq 2} |\tilde{\lambda}_k|^2} \leq \frac{\|\varepsilon\|^2}{\tilde{\lambda}_2^2}.$$

As a result,

$$|\langle \tilde{v}_1, v_1 \rangle|^2 \geq 1 - \frac{\|\varepsilon\|^2}{\tilde{\lambda}_2^2}.$$

Choose α so that $\langle e^{i\alpha} \tilde{v}_1, v_1 \rangle = |\langle \tilde{v}_1, v_1 \rangle|$. Then

$$\begin{aligned} \|v_1 - e^{i\alpha} \tilde{v}_1\|^2 &= 2 - 2\Re \langle e^{i\alpha} \tilde{v}_1, v_1 \rangle \\ &= 2 - 2|\langle \tilde{v}_1, v_1 \rangle| \\ &\leq 2 - 2|\langle \tilde{v}_1, v_1 \rangle|^2 \\ &\leq 2 \frac{\|\varepsilon\|^2}{\tilde{\lambda}_2^2}. \end{aligned}$$

Conclude by multiplying through by n and taking a square root.

2.3 Proof of theorem 4.

The proof follows the argument in section 2.1; we mostly highlight the modifications.

Let $b_i = |b_i|e^{i\phi_i}$. The Laplacian with phases is $\mathcal{L}_b = \Lambda_\phi L_{|b|} \Lambda_\phi^*$, with $\Lambda_\phi = \text{diag}(e^{i\phi_i})$. Explicitly,

$$(\mathcal{L}_b)_{ij} = \begin{cases} \sum_{k:(i,k) \in E} |b_k|^2 & \text{if } i = j; \\ -b_i \bar{b}_j & \text{if } (i, j) \in E; \\ 0 & \text{otherwise,} \end{cases}$$

The matrix $Y = AXA^*$ is compared to the rank-1 spectral projectors of \mathcal{L}_b . We can write it as $Y = bb^* + \tilde{\varepsilon}$ with $\|\tilde{\varepsilon}\|_1 \leq \|\varepsilon\|_1 + \sigma$. The computation of $\langle bb^*, \mathcal{L}_b \rangle$ is now

$$\begin{aligned} \langle bb^*, \mathcal{L}_b \rangle &= \sum_i b_i \bar{b}_i \mathcal{L}_{ii} + \sum_{(i,j) \in E} b_i \bar{b}_j \mathcal{L}_{ij} \\ &= -\sum_i |b_i|^2 \sum_{k:(i,k) \in E} |b_k|^2 + \sum_{(i,j) \in E} b_i \bar{b}_j \bar{b}_i b_j \\ &= \sum_i |b_i|^2 \left[-\sum_{j:(i,j) \in E} |b_j|^2 + \sum_{j:(i,j) \in E} |b_j|^2 \right] \\ &= 0. \end{aligned}$$

The error term is now bounded (in a rather crude fashion) as

$$|\langle \tilde{\varepsilon}, \mathcal{L}_b \rangle| \leq \|\mathcal{L}_b\|_\infty \|\tilde{\varepsilon}\|_1 \leq \left[\max_i \sum_{j:(i,j) \in E} |b_j|^2 \right] \|\tilde{\varepsilon}\|_1 \leq \|b\|^2 \|\tilde{\varepsilon}\|_1.$$

Upon normalizing Y to unit trace, we get

$$|\langle \frac{Y}{\text{tr}(Y)}, \mathcal{L}_b \rangle| \leq \frac{\|b\|^2 \|\tilde{\varepsilon}\|_1}{\|b\|^2 + \text{tr}(\tilde{\varepsilon})} \leq 2\|\tilde{\varepsilon}\|_1,$$

where the last inequality follows from

$$\begin{aligned} |\text{tr}(\tilde{\varepsilon})| &\leq \|\tilde{\varepsilon}\|_1 \\ &\leq \|\varepsilon\|_1 + \sigma \\ &\leq \lambda_2/2 \quad (\text{assumption of the theorem}) \\ &\leq \|b\|^2/2 \quad (\text{by Gershgorin}). \end{aligned}$$

On the other hand, we expand

$$\langle \frac{Y}{\text{tr}(Y)}, \mathcal{L}_b \rangle = \sum_j c_j \lambda_j,$$

and use $X \succeq 0 \Rightarrow Y \succeq 0$ to get $c_j \geq 0$, $\sum_j c_j = 1$. Since $2\|\tilde{\varepsilon}\|_1 \leq \lambda_2$, we conclude as in section 2.1 that

$$\langle \frac{Y}{\text{tr}(Y)}, v_1 v_1^* \rangle \geq 1 - \frac{2\|\tilde{\varepsilon}\|_1}{\lambda_2},$$

hence

$$\|\frac{Y}{\text{tr}(Y)} - v_1 v_1^*\|_F^2 \leq 4 \frac{\|\tilde{\varepsilon}\|_1}{\lambda_2}. \quad (10)$$

For $X = A^+ Y (A^+)^+$, we get

$$\|\frac{X}{\text{tr}(Y)} - (A^+ v_1)(A^+ v_1)^*\|_F^2 \leq 4\|A^+\|^4 \frac{\|\tilde{\varepsilon}\|_1}{\lambda_2}.$$

Call the right-hand side δ^2 . Recall that $v_1 = b/\|b\|$ hence $A^+ v_1 = x_0/\|b\|$. Using $\text{tr}(Y) = \|b\|^2 + \text{tr}(\tilde{\varepsilon})$, we get

$$\|X - x_0 x_0^*\| \leq \delta \text{tr}(Y) + \frac{\|x_0\|^2}{\|b\|^2} |\text{tr}(\tilde{\varepsilon})|. \quad (11)$$

Elementary calculations based on the bound $\|\tilde{\varepsilon}\|_1 \leq \lambda_2/2 \leq \|b\|^2/2$ allow to further bound the above quantity by $\frac{(6+\sqrt{2})}{4} \delta \|b\|^2$. We can now call upon lemma 2, part (b), to obtain

$$\|x\|x\| - e^{i\alpha} x_0 \|x_0\| \leq 2\sqrt{2} \frac{(6+\sqrt{2})}{4} \delta \|b\|^2,$$

where $x = x_1 \sqrt{\lambda_1(X)}$ is the leading eigenvector of X normalized so that $\|x\|^2 = \lambda_1(X)$ is the leading eigenvalue of X . We use (11) one more time to bound

$$|\lambda_1(X) - \|x_0\|^2| \leq \frac{(6+\sqrt{2})}{4} \delta \|b\|^2,$$

hence

$$\begin{aligned} \|x_0\| \|x - e^{i\alpha} x_0\| &\leq \|x\|x\| - e^{i\alpha} x_0 \|x_0\| + \|x\| |\|x\| - \|x_0\|| \\ &\leq 2\sqrt{2} \frac{(6+\sqrt{2})}{4} \delta \|b\|^2 + \frac{\|x\|}{\|x\| + \|x_0\|} |\|x\|^2 - \|x_0\|^2| \\ &\leq (2\sqrt{2} + 1) \frac{(6+\sqrt{2})}{4} \delta \|b\|^2. \end{aligned}$$

Use $\|b\| \leq \|A\| \|x_0\|$ and the formula for δ to conclude that

$$\|x - e^{i\alpha} x_0\| \leq C \|x_0\| \kappa(A)^2 \sqrt{\frac{\|\tilde{\varepsilon}\|_1}{\lambda_2}},$$

with $C = 2(2\sqrt{2} + 1) \frac{(6+\sqrt{2})}{4} \leq 15$.

2.4 Proof of theorem 5.

The proof proceeds as in the previous section, up to equation (10). The rest of the reasoning is a close mirror of the one in the previous section, with Y in place of X , y in place of x , b in place of x_0 , and δ re-set to $2\sqrt{\|\tilde{\varepsilon}\|_1/\lambda_2}$. We obtain

$$\|y - e^{i\alpha} b\| \leq 15 \|b\| \sqrt{\frac{\|\tilde{\varepsilon}\|_1}{\lambda_2}}.$$

We conclude by letting $x = A^+ y$, $x_0 = A^+ b$, and using $\|b\| \leq \|A\| \|x_0\|$.

3 Numerical illustrations

We investigate the scalings of the bounds for phase recovery given by theorems 1 and 3 on toy examples ($n = 2^7$).

3.1 Influence of the spectral gap

We first focus on the scaling with respect to the spectral gap. This is achieved by considering three types of graphs :

- the path P_n which is proven to be the connected graph with the smallest spectral gap⁵;
- graphs obtained by adding randomly K edges to P_n with K ranging from 1 to 50;
- Erdős-Rényi random graphs with probability ranging from 0.03 to 0.05, conditioned on connectedness (positive spectral gap).

A realization of the two latter types of graphs is given in figure 1.

⁵As justified by the decreasing property of λ_2 under edge removal, mentioned earlier.

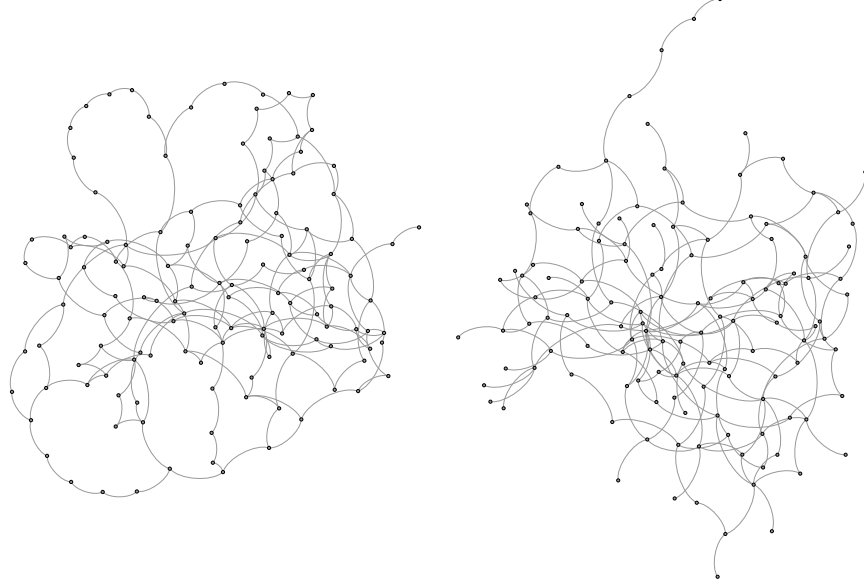


Figure 1: P_n + random edges (left), Erdős-Rényi random graph (right)

To study the eigenvector method, we draw one realization of a symmetric error matrix ε with $\varepsilon_{ij} \sim \mathcal{CN}(0, \eta^2)$, with $\eta = 10^{-8}$. The spectral norm of the noise (used in theorem 3) is $\|\varepsilon\| \sim 2 \times 10^{-7}$.

For different realizations of the aforementioned graphs, we estimate the solution with the eigenvector method and plot the ℓ_2 recovery error as a function of $\tilde{\lambda}_2$. See figure 2.

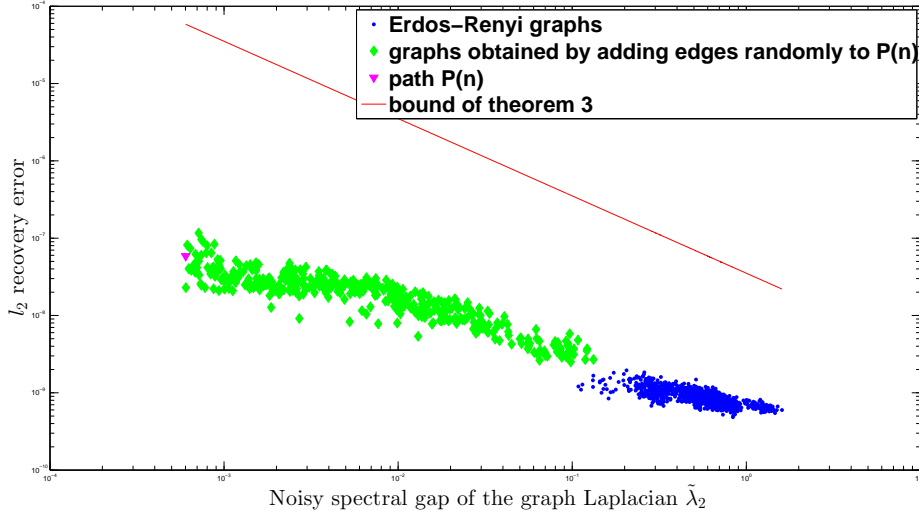


Figure 2: Recovery error for the eigenvector method as a function of $\tilde{\lambda}_2$

To study the feasibility method, we consider the case of an approximate fit ($\sigma = 10^{-4}$) in the noiseless case ($\varepsilon = 0$). The feasibility problem (4) is solved using the Matlab toolbox cvx which calls the toolbox SeDuMi. An interior point algorithm (centering predictor-corrector) is used. The

recovery error as a function of the spectral gap λ_2 is illustrated in figure 3.

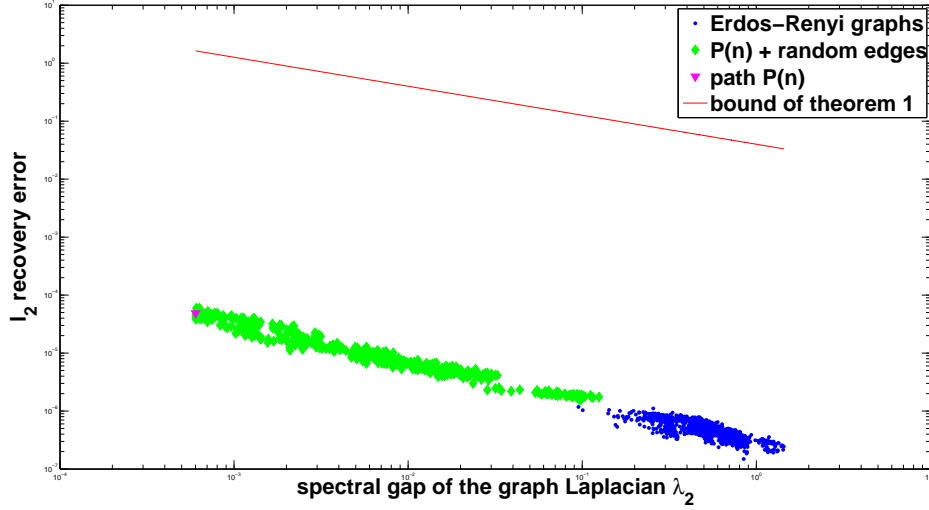


Figure 3: Recovery error for the feasibility method as a function of λ_2

3.2 Influence of the noise level

We now fix the set E as one realization of adding $K = 15$ edges randomly to P_n . We then draw realizations of the noise level, $\varepsilon \sim \mathcal{CN}(0, \eta^2)$ with η logarithmically equally spaced between $10^{-6}\lambda_2$ and $10^{-1}\lambda_2$. The recovery for the eigenvector method is illustrated in figure 4.

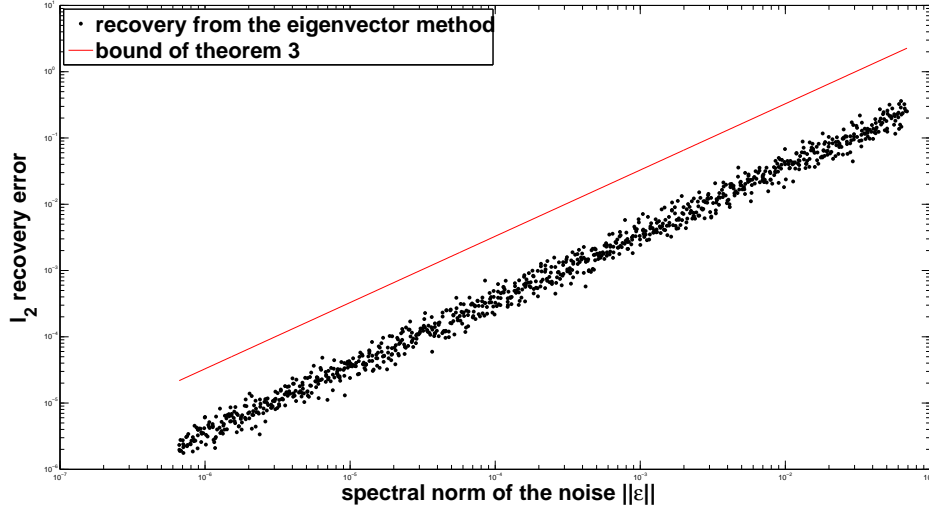


Figure 4: Recovery error for the eigenvector method as a function of the spectral norm of the noise $\|\varepsilon\|$

For the feasibility problem, we chose σ to be two times the ℓ_1 norm of ϵ on E . The recovery for the feasibility method is illustrated in figure 5. As mentioned earlier, it is unclear to us whether

the bound could be strengthened or if the discrepancy owes to the particular method by which a point is chosen in the feasibility set.

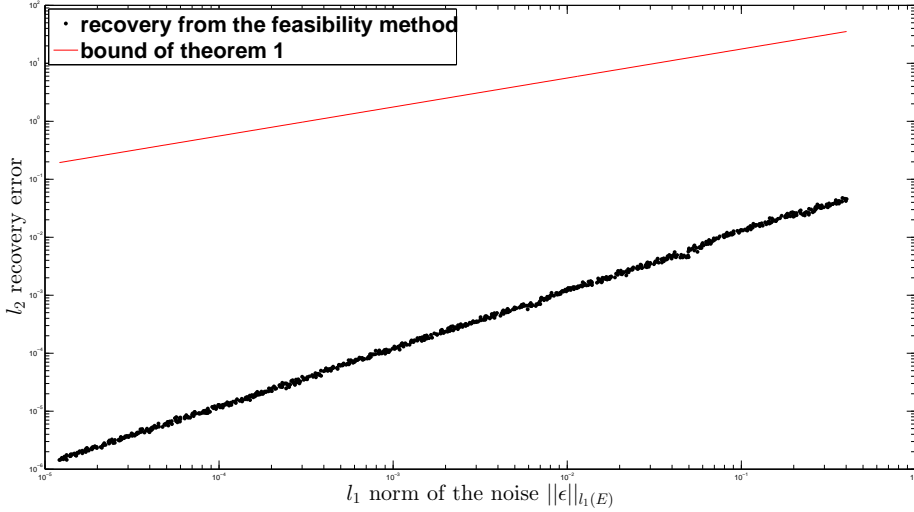


Figure 5: Recovery error for the feasibility method as a function of the l_1 norm of the noise $\|\epsilon\|_1$.

3.3 Interferometric inverse scattering

An important application of interferometric ideas is to the inversion of a medium's index of refraction from recordings of waves scattered by that medium, as in seismic imaging.

In a first numerical experiment, we let $b = Ax$ where x is a reflectivity profile in a rectangle (perturbation of the index of refraction), and A is an acoustic wave equation that maps this reflectivity profile in a linearized way to the solution wavefield b sampled at receivers placed at the top edge of the rectangle (surface). The wave equation is discretized via finite differences, with different schemes for the data modeling step and for the inversion step. The data index i runs over receiver locations x_r , frequencies ω , and source positions x_s (which define different wave equations with different right-hand sides.) Figure 6 shows robust recovery of x from noisy b , both by least-squares and by interferometric inversion. Here the noise model is taken to be Gaussian,

$$\tilde{b}_i = b_i + \eta_i \quad \eta_i \sim \mathbb{CN}(0, \sigma^2)$$

where \mathbb{CN} is the complex normal distribution and $\sigma = 0.1 \frac{\|b\|_2}{\sqrt{2n}}$ so that $\frac{\|\eta\|_2}{\|b\|_2} = 0.1$ (10% additive noise).

In this case the graph E is taken to be an Erdős-Rényi random graph with $p = 1.5 \frac{\log(N)}{N}$ to ensure connectedness. The computational method used for handling this example is a rank-2 relaxation scheme explained in the companion note [14].

In a second numerical experiment, we show that interferometric inversion is still accurate and stable, even when the forward model $b = \mathcal{A}(x)$ is the full wave equation that maps the index of refraction x to the wavefield b nonlinearly (no Born approximation.) Again, 10% Gaussian noise is added. Figure 7 shows the result of nonlinear least-squares inversion, and the corresponding interferometric inversion result.

These numerical experiments merely show that interferometric inversion can be accurate and stable under minimal assumptions on the graph E of data pair products. One rationale for switching to the interferometric formulation is that its results display robustness vis-a-vis uncertainties *in the forward model A* , an aspect that we briefly document in [14] and intend to further investigate.

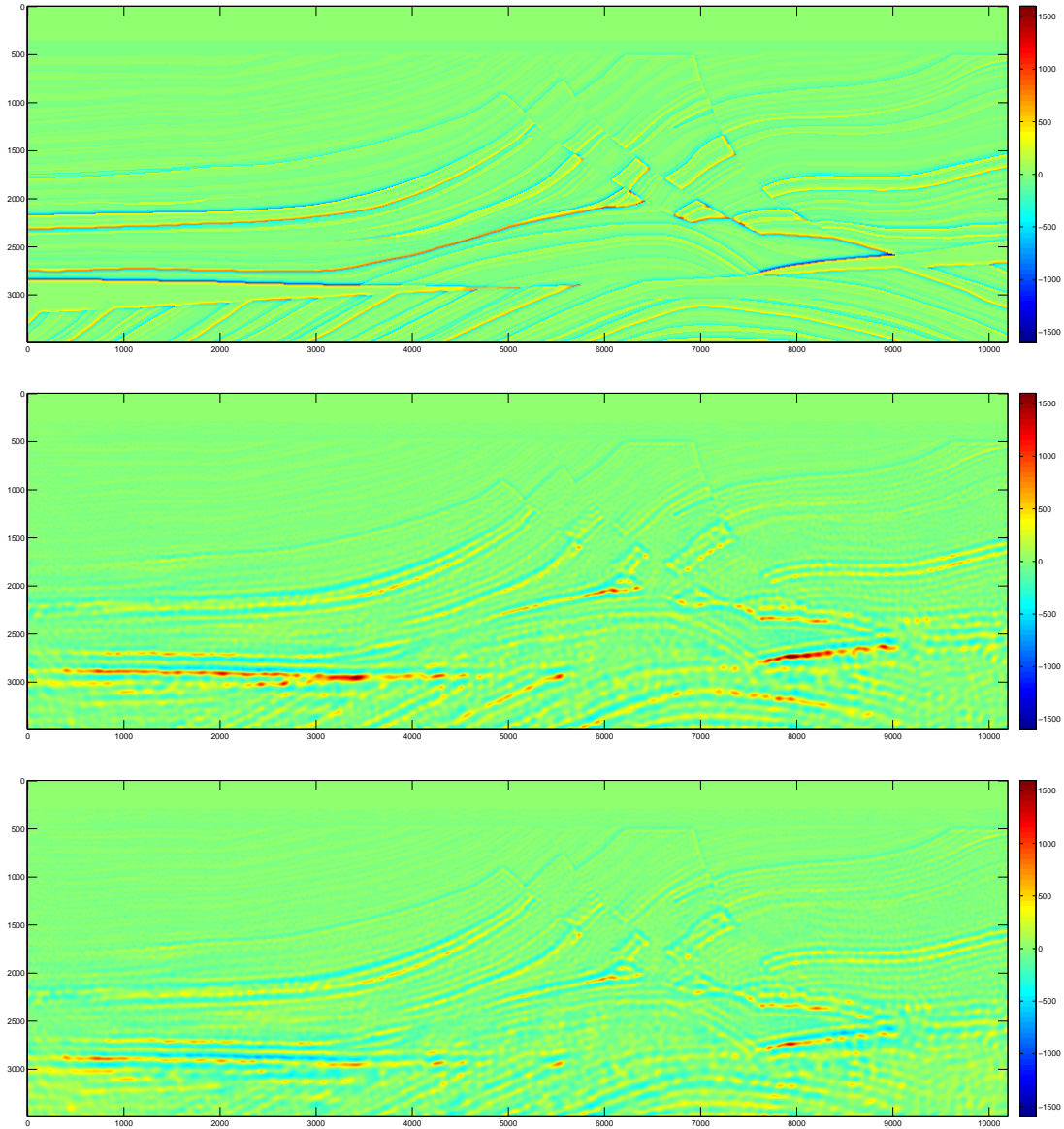


Figure 6: First: true, unknown reflectivity profile x . Second: least-squares solution. Third: result of interferometric inversion.

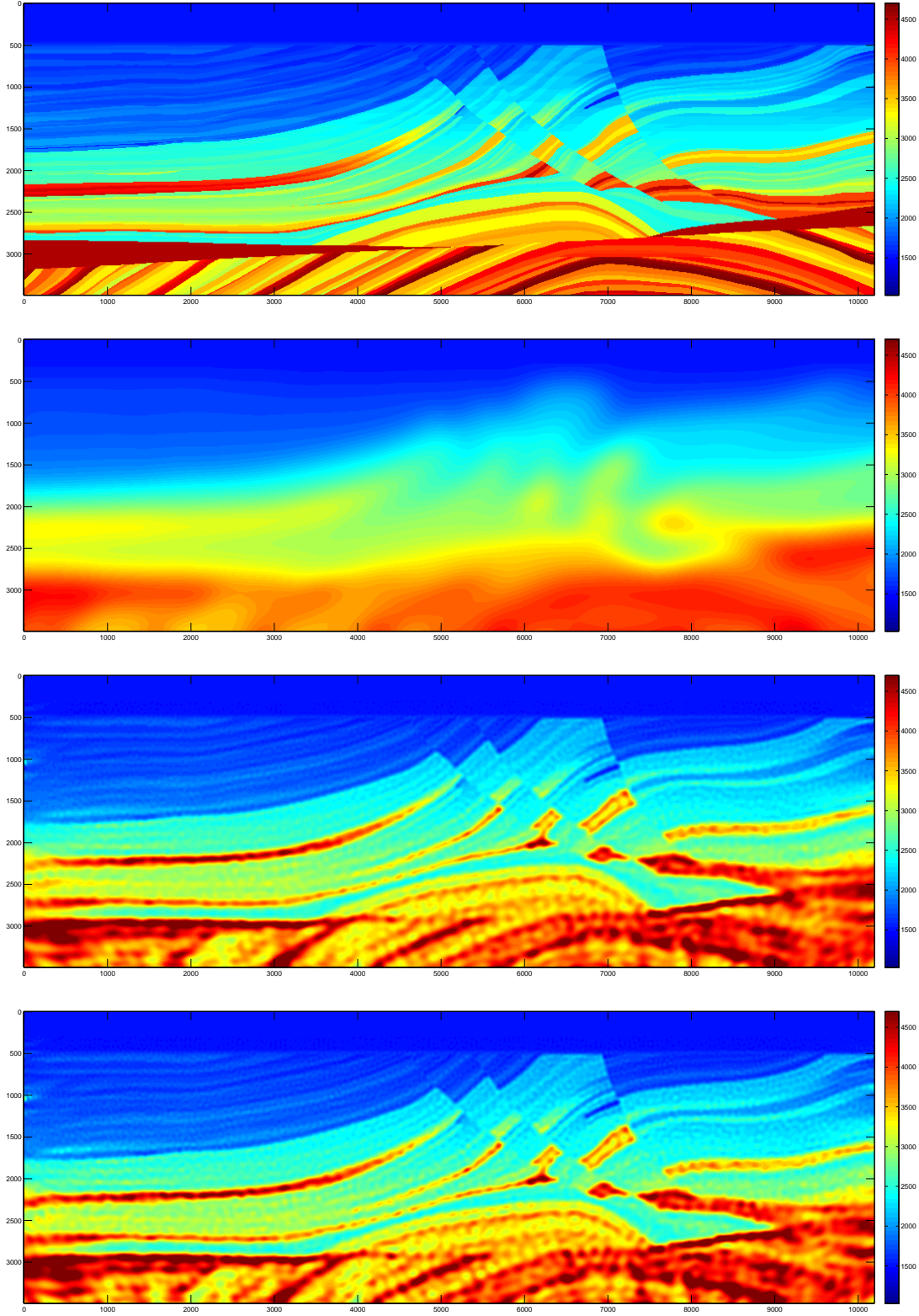


Figure 7: First: true, unknown map of the index of refraction x . Second: initial guess for either inversion scheme. Third: nonlinear least-squares solution. Fourth: result of interferometric inversion.

References

- [1] B. Alexeev, A. S. Bandeira, M. Fickus and D. G. Mixon. Phase retrieval with polarization, *arXiv preprint arXiv:1210.7752*, 2012
- [2] A. S. Bandeira, A. Singer, and D. A. Spielman. A Cheeger inequality for the graph connection Laplacian, *arXiv preprint arXiv:1204.3873*, 2012
- [3] P. Blomgren, G. Papanicolaou, and H. Zhao, Super-resolution in time-reversal acoustics, *J. Acoust. Soc. Am.* 111(1), 230-248, 2002
- [4] L. Borcea, G. Papanicolaou, and C. Tsogka, Interferometric array imaging in clutter, *Inv. Prob.* 21(4), 1419-1460, 2005
- [5] E. J. Candes, Y. C. Eldar, T. Strohmer and V. Voroninski. Phase retrieval via matrix completion, *SIAM Journal on Imaging Sciences*, 6(1), 199-225, 2013
- [6] E. J. Candes, B. Recht, Exact Matrix Completion via Convex Optimization, *Found. Comput. Math.*, 9-6, 717-772, 2009
- [7] A. Chai, M. Moscoso, and G. Papanicolaou. Array imaging using intensity-only measurements, *Inverse Problems* 27.1 015005, 2011
- [8] S. Chatterjee, Matrix estimation by Universal Singular Value Thresholding, *arXiv preprint arXiv:1212.1247*, 2012
- [9] L. Demanet and P. Hand. Stable optimizationless recovery from phaseless linear measurements, *preprint*, 2013
- [10] E. Dussaud, *Velocity analysis in the presence of uncertainty*, Ph.D. thesis, Computational and Applied Mathematics, Rice University, 2005
- [11] J. Garnier, Imaging in randomly layered media by cross-correlating noisy signals, *SIAM Multiscale Model. Simul.* 4, 610-640, 2005
- [12] M. Goemans and D. Williamson, Improved approximation algorithms for maximum cut and satisfiability problems using semidefinite programming, *Journal of the ACM*, 42(6), 1115-1145, 1995
- [13] A. Javanmard, A. Montanari, Localization from incomplete noisy distance measurements, *Found. Comput. Math.* 13, 297-345, 2013
- [14] V. Jugnon and L. Demanet, Interferometric inversion: a robust approach to linear inverse problems, to appear in *Proc. SEG Annual Meeting*, 2013
- [15] R. Keshavan, A. Montanari, S. Oh, Matrix Completion from Noisy Entries, *Journal of Machine Learning Research* 11, 2057-2078, 2010
- [16] O. I. Lobkis and R. L. Weaver, On the emergence of the Greens function in the correlations of a diffuse field, *J. Acoustic. Soc. Am.*, 110, 3011-3017, 2001
- [17] L. Lovasz, *Eigenvalues of graphs*, Lecture notes, 2007
- [18] B. Recht, M. Fazel, and P. A. Parrilo. Guaranteed minimum-rank solutions of linear matrix equations via nuclear norm minimization, *SIAM Review* 52-3, 471-501, 2010

- [19] J. M. Rodenburg, A. C. Hurst, A. G. Cullis, B. R. Dobson, F. Pfeiffer, O. Bunk, C. David, K. Jefimovs, and I. Johnson. Hard-x-ray lensless imaging of extended objects, *Physical review letters* 98, no. 3 034801, 2007
- [20] J. Schotland, Quantum imaging and inverse scattering, *Optics letters*, 35(20), 3309-3311, 2010
- [21] G. T. Schuster, *Seismic Interferometry* Cambridge University Press, 2009
- [22] G. T. Schuster, J. Yu, J. Sheng, and J. Rickett, Interferometric/daylight seismic imaging *Geophysics* 157(2), 838-852, 2004
- [23] A. Singer. Angular synchronization by eigenvectors and semidefinite programming, *Applied and computational harmonic analysis* 30.1 20-36, 2011
- [24] A. Singer, M. Cucuringu, Uniqueness of low-rank matrix completion by rigidity theory, *SIAM. J. Matrix Anal. Appl.* 31(4), 16211641, 2010
- [25] L. Wang and A. Singer. Exact and Stable Recovery of Rotations for Robust Synchronization, *arXiv preprint arXiv:1211.2441*, 2012
- [26] I. Waldspurger, A. d’Aspremont, S. Mallat, Phase recovery, maxcut and complex semidefinite programming, *arXiv preprint arXiv:1206.0102* 2012
- [27] K. Wapenaar and J. Fokkema, Greens function representations for seismic interferometry, *Geophysics*, 71, SI33-SI46, 2006